

# Dimethyl sulfide acts as eat-me signal during microbial predator-prey interactions in the ocean

**Adva Shemi**

The Weizmann Institute of Science

**Uria Alcolombri**

ETH Zurich <https://orcid.org/0000-0003-3561-5091>

**Daniella Schatz**

Weizmann Institute of Science <https://orcid.org/0000-0003-2740-8391>

**Viviana Farstey**

The Interuniversity Institute for Marine Sciences

**Ron Rotkopf**

Weizmann Institute of Science <https://orcid.org/0000-0001-9503-7348>

**Shifra Ben-Dor**

Weizmann Institute of Science <https://orcid.org/0000-0001-9604-1939>

**Miguel Frada**

The Interuniversity Institute of Eilat <https://orcid.org/0000-0001-8287-0795>

**Dan Tawfik**

Weizmann Institute of Science <https://orcid.org/0000-0002-5914-8240>

**Assaf Vardi** (✉ [assaf.vardi@weizmann.ac.il](mailto:assaf.vardi@weizmann.ac.il))

Weizmann Institute of Science <https://orcid.org/0000-0002-7079-0234>

---

## Research Article

**Keywords:** Oceanic Carbon and Sulfur Cycles, Bloom Events, Chemoattraction, Prey Cells, *Emiliania huxleyi*, *Oxyrrhis marina*

**Posted Date:** January 22nd, 2021

**DOI:** <https://doi.org/10.21203/rs.3.rs-139243/v1>

**License:**  This work is licensed under a Creative Commons Attribution 4.0 International License.

[Read Full License](#)

---

**Version of Record:** A version of this preprint was published at Nature Microbiology on October 25th, 2021. See the published version at <https://doi.org/10.1038/s41564-021-00971-3>.



1 **Dimethyl sulfide acts as eat-me signal during microbial predator-prey interactions in**  
2 **the ocean**

3  
4 Adva Shemi<sup>1</sup>, Uria Alcolombri<sup>1,2</sup>, Daniella Schatz<sup>1</sup>, Viviana Farstey<sup>3</sup>, Ron Rotkopf<sup>4</sup>, Shifra  
5 Ben-Dor<sup>4</sup>, Miguel J. Frada<sup>3,5</sup>, Dan S. Tawfik<sup>6</sup>, Assaf Vardi<sup>1\*</sup>

6 <sup>1</sup>Department of Plant and Environmental Sciences, Weizmann Institute of Science,  
7 Rehovot 7610001, Israel.

8 <sup>2</sup>Institute of Environmental Engineering, Department of Civil, Environmental and  
9 Geomatic Engineering, ETH Zurich, Zurich, Switzerland.

10 <sup>3</sup>The Interuniversity Institute for Marine Sciences, Eilat 8810302, Israel.

11 <sup>4</sup>Department of Life Sciences Core Facilities, Weizmann Institute of Science, Rehovot  
12 7610001, Israel.

13 <sup>5</sup>Department of Ecology, Evolution and Behavior, Alexander Silberman Institute of Life  
14 Sciences, Hebrew University of Jerusalem, Jerusalem 91904, Israel.

15 <sup>6</sup>Department of Biomolecular Sciences, Weizmann Institute of Science, 7610001  
16 Rehovot, Israel.

17 \*Corresponding author. E-mail: [assaf.vardi@weizmann.ac.il](mailto:assaf.vardi@weizmann.ac.il) (A.V.)

18  
19 **Summary**

20 Phytoplankton are key components of the oceanic carbon and sulfur cycles <sup>1</sup>. During bloom  
21 events, some species can emit massive amounts of the organosulfur volatile dimethyl  
22 sulfide (DMS) to the atmosphere, where it can modulate aerosol formation and affect  
23 climate <sup>2,3</sup>. In aquatic environments, DMS plays an important role as a chemical signal  
24 mediating diverse trophic-level interactions. Yet its role in microbial predator-prey  
25 interactions remains elusive with contradicting evidence for its role in algal chemical  
26 defense and in grazer's chemoattraction to prey cells <sup>4-6</sup>. Here, we investigated the signaling  
27 role of DMS during zooplankton-algae interactions by genetic and biochemical  
28 manipulation of the algal DMS-generating enzyme (Dimethylsulfoniopropionate lyase,  
29 DL) from the bloom-forming alga *Emiliania huxleyi* <sup>7</sup>. We inhibited DL activity in live *E.*  
30 *huxleyi* cells by the novel DL-inhibitor 2-bromo-3-(dimethylsulfonio)-propionate (Br-  
31 DMSP) <sup>8</sup>, and overexpressed DL in the model diatom *Thalassiosira pseudonana*. We  
32 showed that algal DL activity did not serve as anti-grazing chemical defense, and  
33 paradoxically enhanced grazing by the model microzooplankton *Oxyrrhis marina* and  
34 other micro- and mesozooplankton, including ciliates and copepods. Consumption of algal  
35 prey with induced DL activity also promoted *O. marina*'s growth. Overall, our results  
36 demonstrate that DMS-mediated herbivory may be ecologically important and prevalent

37 during prey-predator dynamics in oceanic ecosystems. The role of algal DMS acting as eat-  
38 me signal to grazers revealed here raises fundamental questions regarding the retention of  
39 its biosynthetic enzyme through the evolution of dominant bloom-forming phytoplankton  
40 in the ocean.

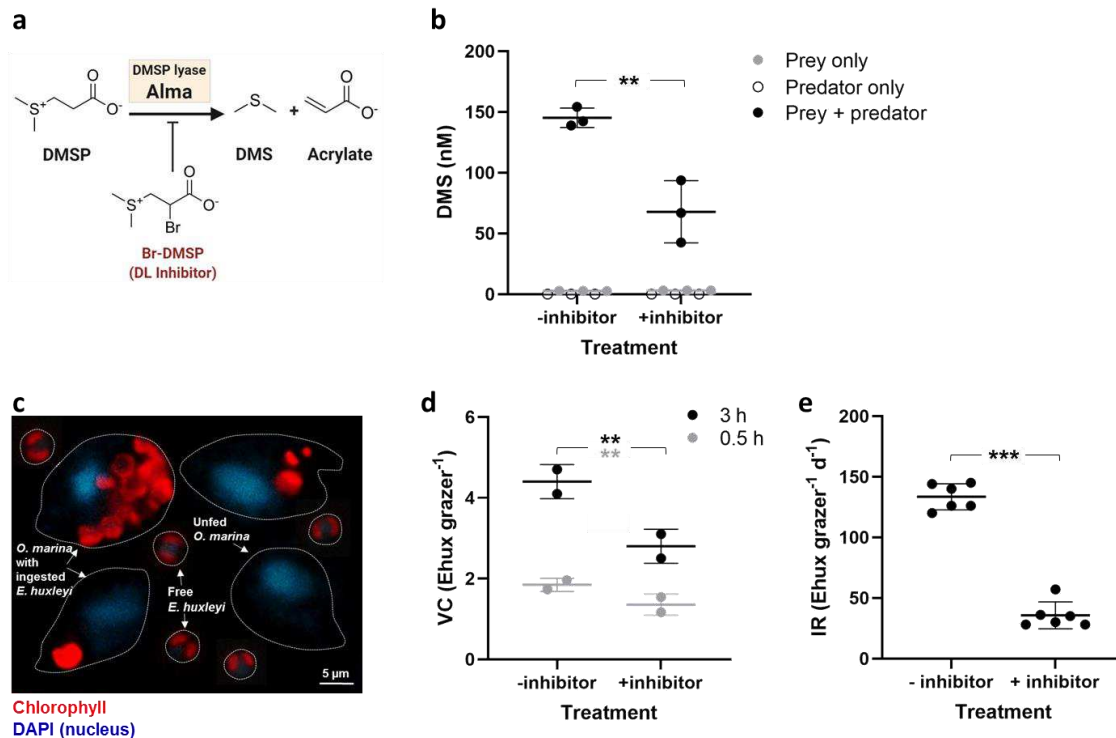
41

42 The ocean is the main source of atmospheric dimethyl sulfide (DMS), with an estimated  
43 flux of 13 to 37 Tg S year<sup>-1</sup> <sup>1,9</sup>. The gaseous DMS is a precursor of sulfate aerosols,  
44 mediating cloud condensation and promoting a cooling effect on Earth's climate <sup>1,2,10</sup>. DMS  
45 is produced by marine phytoplankton through cleavage of the zwitterionic organosulfur  
46 compound dimethylsulfoniopropionate (DMSP) by the DMSP lyase (DL) enzyme <sup>11-13</sup>. In  
47 phytoplankton, DMSP was proposed to act as an intracellular osmoprotectant, antioxidant  
48 and energy dissipation factor <sup>14-16</sup>. In addition, both DMSP and DMS were also shown to  
49 act as infochemicals (chemical cues that facilitate communication), mediating virulence  
50 or symbiosis by bacteria (for DMSP) <sup>17,18</sup>, and promoting prey-predator interaction and  
51 parasite infection (for DMS) <sup>19</sup>. Notably, marine predators including invertebrates, sea  
52 birds and whales, can sense DMS and track it to find areas of high productivity <sup>20-24</sup>.  
53 Although DMS is highly produced via DMSP lyase (DL) in grazed algal cells <sup>25</sup>, its  
54 signaling role during phytoplankton and zooplankton interactions is still unresolved. Two  
55 contradictory roles were proposed for DMS and its precursor DMSP, as anti-grazing  
56 defense <sup>4,26</sup> and pro-grazing chemoattractant <sup>6</sup>. We aimed to unravel this debate by  
57 combining functional genomics and physiological approaches to assess the impact of DMS  
58 during zooplankton-algae interactions. We used the bloom-forming cosmopolitan  
59 coccolithophore *Emiliana huxleyi* (Prymnesiophyceae) from which a DL enzyme was  
60 recently isolated (Alma1) <sup>7,27-29</sup>. The full characterization of Alma1 and its conservation  
61 among diverse taxa<sup>7</sup> provided a unique opportunity to unravel its ecophysiological role.  
62 We directly manipulated DL activity in prey cells in order to determine the influence of  
63 DMS on grazing dynamics by zooplankton, focusing on microzooplankton.  
64 Microzooplankton (20-200 μm) are key marine herbivores that remove 49-77% of the  
65 photosynthetic biomass daily <sup>30-32</sup> and in fact DMS is often produced via DL activity upon  
66 disruption of algal cells during grazing <sup>25</sup>. Here, we demonstrate that DMS enhances  
67 grazing efficiency by micro- and mesozooplankton, and further discussed the ecological  
68 and evolutionary implications of DMS-mediated herbivory in the ocean.

69

70 We firstly examined the effect of DMS emission on grazing dynamics between *E. huxleyi*  
71 high DL strain CCMP373 and *Oxyrrhis marina*, a heterotrophic dinoflagellate commonly  
72 used as a model microzooplankton <sup>33</sup>. In order to directly link between algal DMS and  
73 grazing efficiency, we applied a novel selective DL-inhibitor, 2-bromo-3-  
74 (dimethylsulfonio)-propionate (Br-DMSP) which blocked *E. huxleyi*'s DL activity *in-vitro*  
75 <sup>8</sup>. During short-term grazing experiments in the presence of 0.2 μM Br-DMSP, DMS  
76 release to the culture medium from grazed cells decreased by ~50%, compared to control

77 culture (Fig. 1a,b and Supplementary Fig. 1). Imaging of the grazer's food vacuole by  
 78 fluorescence microscopy revealed that inhibition of DL activity led to > 50% reduction in  
 79 prey content as compared to ingestion of control cells after 0.5 and 3 h of predation (Fig.  
 80 1c,d). Furthermore, the ingestion rate on Br-DMSP treated cells declined by ~74% (~35 *E.*  
 81 *huxleyi* grazer<sup>-1</sup> day<sup>-1</sup>) as compared to untreated control cells (~133 *E. huxleyi* grazer<sup>-1</sup> day<sup>-1</sup>),  
 82 based on quantification of prey clearance by flow-cytometry (Fig. 1e). Notably, even  
 83 partial inhibition of DL activity led to pronounced reduction in grazing rate. As a control  
 84 for a possible indirect effect of Br-DMSP, we used the green alga *Dunaliella tertiolecta* as  
 85 prey since it lacks the DL enzyme. Indeed, no change was detected in the consumption of  
 86 *D. tertiolecta* by *O. marina* in the presence of Br-DMSP (Supplementary Table 1).



87

88 **Fig 1. Reduced DMSP lyase (DL) activity of *E. huxleyi* impaired grazing by *O. marina*.** a, The  
 89 DMSP lyase Alma cleaves DMSP to DMS and acrylate. The inhibitor Br-DMSP blocks DL activity  
 90 by forming an enzyme-inhibitor covalent bond at the active site, thus inhibiting the formation of  
 91 DMS and acrylate<sup>8</sup>. b, The short-term (~1 h) effect of 0.2 μM Br-DMSP on DMS production *in-*  
 92 *vivo* by *E. huxleyi* 373. Horizontal lines represent the mean ± SD; *n* = 3; *P* < 0.008 (Student's T-  
 93 test). c, Fluorescence micrograph collage of *O. marina* with free and ingested *E. huxleyi* cells at  
 94 *t*=30 minutes from prey addition. d, The effect of 0.2 μM Br-DMSP on the food vacuole content  
 95 (VC, *E. huxleyi* 373 cells per grazer) of *O. marina* at *t*=0.5 and 3 h. A total of 800 *O. marina* cells  
 96 were examined, 100 cells per biological replicate. Horizontal lines represent the mean ± SD; *n* = 2;  
 97 *P* < 0.003 (generalized linear mixed model). e, The effect of 0.2 μM Br-DMSP on ingestion rate  
 98 (IR) of *E. huxleyi* 373 cells (Ehux) by *O. marina*, quantified by flow cytometry and based on prey  
 99 removal from the medium during 50 min. Approximately 2,500 cells were analyzed per sample.  
 100 Horizontal lines represent the mean ± SD; *n* = 6; *P* < 0.0001 (Student's T-test).

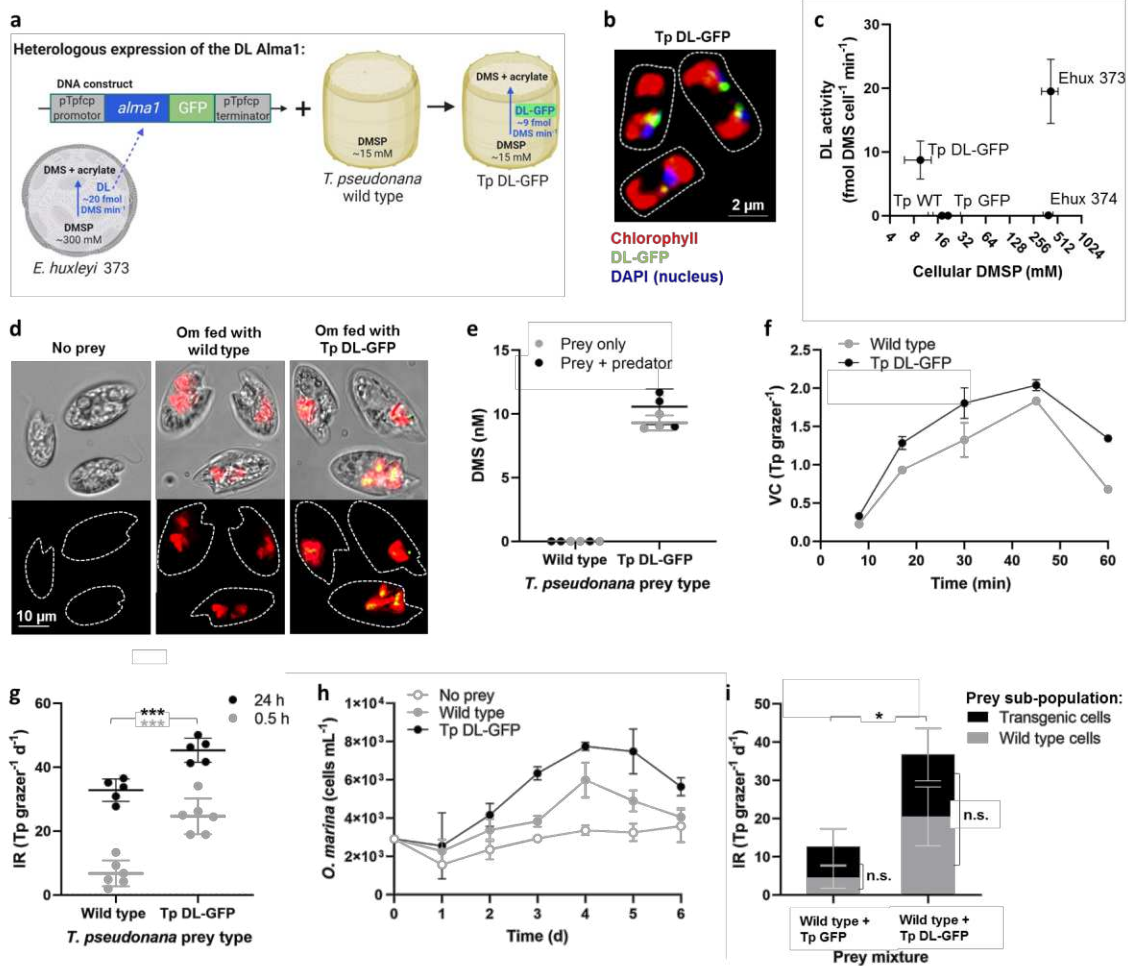
101

102 *E. huxleyi* cells produce minimal amounts of DMS during exponential growth (Fig. 1b and  
103 Supplementary Fig. 2), probably because the DL and its substrate DMSP are segregated in  
104 different subcellular compartments<sup>34</sup>. However, algal senescence and interactions with  
105 viruses<sup>11,35</sup>, and as we show here with grazers (Fig. 1b and Supplementary Fig. 2), trigger  
106 DL activity and significant DMS production, probably as a result of damaged cellular  
107 membranes and mixing of DL and DMSP<sup>36-38</sup>. Here, inhibition of the prey's DL activity  
108 suppressed grazing efficiency by *O. marina*. Hence, we hypothesize that increasing DL  
109 activity will enhance the grazing response by microzooplankton. Exogenous application of  
110 DMS or acrylate (the products of DL activity, Fig. 1a) to *E. huxleyi* strain CCMP2090,  
111 which has low DL activity and produces no detectable DMS, did not significantly alter the  
112 grazing response by *O. marina* (Supplementary Fig. 3). It is likely that bulk addition failed  
113 to mimic the natural spatiotemporal DMS gradients in seawater and in the cell's  
114 microenvironment. Thus, the cellular release of infochemicals during microbial  
115 interactions may be critical for understanding their signaling role. In order to directly  
116 address the biological context of DMS release, genetic manipulation of the DL enzyme in  
117 prey cells is critical. As *E. huxleyi* and other major DMS producing species are yet to be  
118 genetically amenable, we conducted heterologous expression of the *E. huxleyi* DL gene  
119 in the ecologically important diatom species *Thalassiosira pseudonana*<sup>39-42</sup>. *T.*  
120 *pseudonana* is similar in size to *E. huxleyi* (3-5  $\mu\text{m}$ ) and synthesizes DMSP ( $\sim 10 \text{ mM cell}^{-1}$ )<sup>43</sup>,  
121 but lacks a DMSP lyase and does not produce DMS<sup>7,43</sup>. Thus, transgenic *T.*  
122 *pseudonana* can serve as a tractable model system to study the direct signaling role of DMS  
123 during grazing interactions. We overexpressed the DMSP lyase encoding gene from *E.*  
124 *huxleyi* 373 (*alma1*) in *T. pseudonana* and fused it to GFP at the C-terminus in order to  
125 preserve a putative target sequence at the N-terminus (Fig. 2a,b and Supplementary Fig.  
126 4). The heterologous expression of the *E. huxleyi* DL in a transgenic *T. pseudonana* line,  
127 called Tp DL-GFP, was verified by western blot using an antibody raised against the Alma1  
128 protein (Supplementary Fig. 4b). DL enzymatic activity in Tp DL-GFP cell lysate ( $8.8 \pm$   
129  $2.9 \text{ fmol DMS cell}^{-1} \text{ min}^{-1}$ , Fig. 2c) was comparable to *E. huxleyi* high DL strains<sup>7,44</sup>. Both  
130 the morphology and growth dynamic of the transgenic cells were not affected by the  
131 expression of Alma1-GFP (Supplementary Fig. 5). Live Tp DL-GFP cells produced DMS  
132 levels comparable to those found in seawater samples ( $\sim 9 \text{ nM}$ )<sup>45,46</sup>. We did not detect,  
133 however, a significant increase in DMS concentration during grazing by *O. marina* in Tp  
134 DL-GFP (Fig. 2d,e). The *in-vivo* DMS production in grazed Tp DL-GFP cells was  
135 predicted to be limited by the considerably lower intracellular levels of DMSP in *T.*  
136 *pseudonana* relative to *E. huxleyi* (Fig. 2c).

137 In order to investigate the direct effect of enhanced DL activity on grazing efficiency, we  
138 conducted feeding experiments with *O. marina* using Tp DL-GFP cells as prey. Grazers  
139 fed with Tp DL-GFP accumulated significantly more prey in their food vacuole over time  
140 (Fig. 2f). In accordance, the ingestion rate on Tp DL-GFP cells was  $\sim 2$ -4 fold higher than  
141 on wild type cells ( $24 \pm 5$  and  $6 \pm 4 \text{ T. pseudonana grazer}^{-1} \text{ day}^{-1}$  during the first 30 min,

142 respectively. Fig. 2g and Supplementary Fig. 6). Furthermore, ingestion by *O. marina* was  
143 also elevated during grazing *T. pseudonana* expressing only DL (Tp DL), while ingestion  
144 of *T. pseudonana* expressing only GFP (Tp-GFP) was similar to wild type (Supplementary  
145 Fig. 7c and 6b). This eliminates the possibility that the prey's GFP fluorescence modulated  
146 grazing activity, and indicates that enhanced grazing on Tp DL-GFP was solely due to the  
147 induced DMS production. Intriguingly, daily feeding on Tp DL-GFP cells significantly  
148 improved *O. marina* growth, as compared with a wild type diatom diet (Fig. 2h). Thus, DL  
149 activity in prey cells not only expedited grazing dynamics, but also enhanced the grazer's  
150 growth on a longer timescale. This may be attributed to general higher consumption of  
151 algal biomass and to specific assimilation of the diatom's DMSP as an essential nutritious  
152 sulfur<sup>47</sup>.

153 In order to further examine if *O. marina* preferentially ingested DMS-producing cells, or  
154 alternatively whether the diffusible DMS may elicit a general unselective grazing activity,  
155 we conducted double-prey competition trials. The total ingestion rate of cells in a prey  
156 mixture containing Tp DL-GFP and wild type cells (1:1) was over ~2 fold higher as  
157 compared to ingestion on a mixture of wild type cells with Tp GFP (Fig. 2i). This indicated  
158 that DMS formed by DL activity in grazed cells can increase the grazing likelihood of  
159 neighboring cells with no DL activity. Therefore, DMS can potentially enhance grazing  
160 within natural algal communities where only a fraction of the cells secretes DMS. Indeed,  
161 during the double-prey competition trials there was no significant difference between the  
162 uptake of each prey type (wild type or Tp DL-GFP), and no preference by *O. marina*  
163 towards Tp DL-GFP cells (Fig. 2i). Thus, *O. marina* grazing on Tp DL-GFP was non-  
164 selective, and may be attributed to dissolved chemical signals such as DMS, which acts as  
165 an appetizing infochemical enhancing general grazing activity.



166

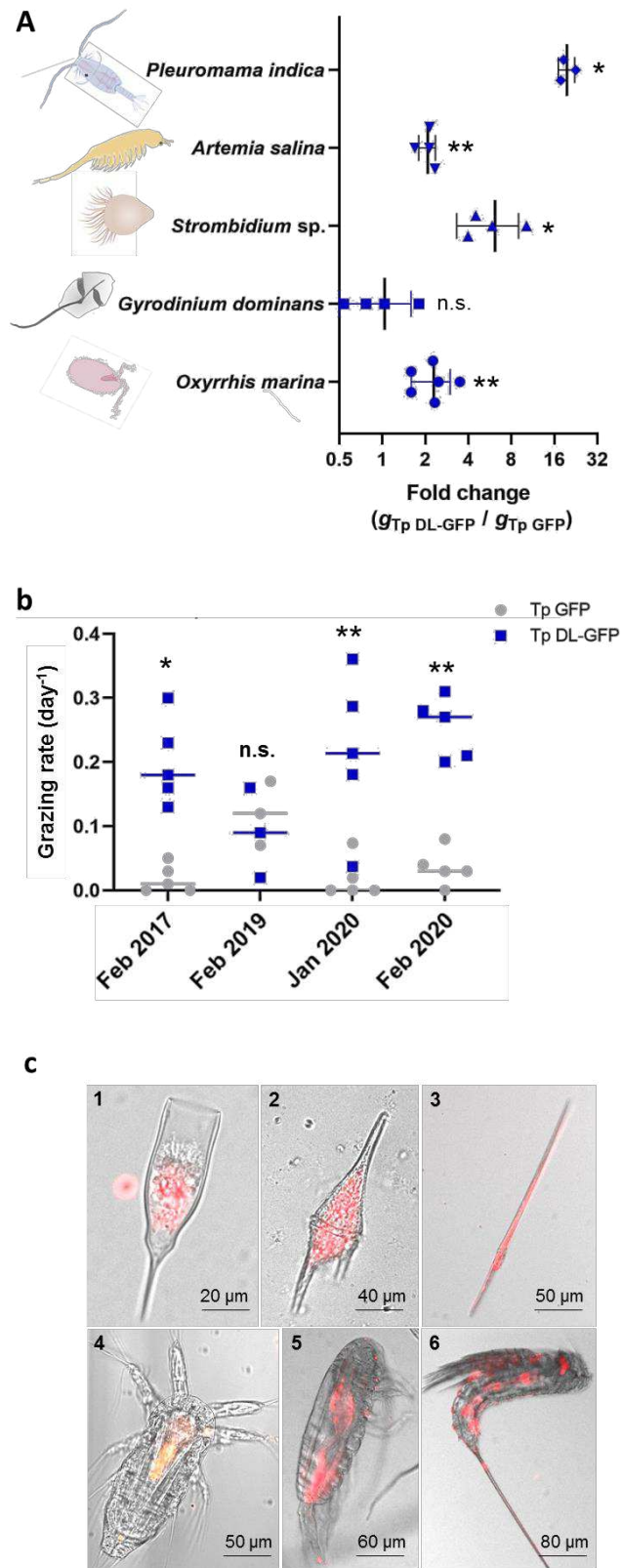
167 **Fig. 2. Overexpression of DMSP lyase (DL) in algal prey cells enhanced grazing efficiency**  
 168 **and growth by *O. marina*.** **a**, Transgenic Tp DL-GFP cells were generated by heterologous  
 169 expression of the *alma1* gene from *E. huxleyi* 373, fused to GFP, in wild type *T. pseudonana* cells.  
 170 **b**, Confocal microscopy of Tp DL-GFP cells. The Alma-GFP protein can be observed as a punctate  
 171 green signal in close proximity to the chloroplast. **c**, Intracellular DMSP content and DL activity in  
 172 *E. huxleyi* (Ehux) strains 373 and 374, as well as in *T. pseudonana* wild type (Tp WT), Tp GFP and  
 173 Tp DL-GFP. We quantified DL activity *in vitro* by measuring DMS generation in cell lysates  
 174 following addition of 10 mM DMSP. Values are mean  $\pm$  SD;  $n = 3-4$ . For DMSP, results from two  
 175 independent measurements were averaged. **d**, Bright field and fluorescence micrographs of *O.*  
 176 *marina* (Om) with ingested *T. pseudonana* cells. **e**, DMS emission during grazing by *O. marina*  
 177 on Tp DL-GFP cells. Horizontal lines represent the mean  $\pm$  SD;  $n = 3$ . **f**, Prey uptake curve based on  
 178 vacuole content (VC) analysis during the first hour of grazing interaction. Values represent the  
 179 mean  $\pm$  SD.  $n = 2-4$ . A total of 800 grazers were analyzed for  $t = 8$  and 17 min, and 400 grazers for  
 180  $t = 30, 45$ , and 60 min. The mean VC values during 60 min were significantly different between the  
 181 two prey types,  $P < 0.0001$  (generalized linear mixed model). **g**, Ingestion rate (IR) analysis based  
 182 on quantification of *T. pseudonana* (Tp) cell removal from the medium during 0.5 and 24 h of  
 183 incubation with *O. marina*. Horizontal lines represent the mean  $\pm$  SD;  $n = 6$ .  $P < 0.0001$  (Student's  
 184 T-test). **h**, Growth dynamics of *O. marina* under starvation conditions or daily feeding with Tp DL-  
 185 GFP or wild type cells;  $n = 4$ . The growth in the Tp DL-GFP treatment was significantly faster than  
 186 wild type,  $P < 0.0012$  (mixed effects model). **i**, Double-prey competition trials based on IR analysis  
 187 of two prey types introduced to *O. marina* in a 1:1 ratio, as measured over 2 h. Values are mean  $\pm$

188 SD;  $n = 3-4$  in two independent experiments.  $P < 0.001$  when comparing the total IR between the  
189 two prey mixtures. When comparing the specific IR on each prey sub-population within a mixture,  
190  $P > 0.32$ , n.s.- not significant (Student's T-test).

191

192 In order to explore the prevalence of DL-mediated herbivory, grazing assays were  
193 conducted with microzooplankton from different taxa, size and feeding modes (i.e. direct  
194 engulfment or filter feeding. Fig. 3a and Supplementary Table 2). The fold-change between  
195 the grazing rate on Tp DL-GFP and Tp GFP cells, which differ only by their DL activity,  
196 was calculated for each grazer species (if the fold-change  $>1$ , DL-GFP cells were  
197 consumed faster than Tp GFP cells). As thecate dinoflagellates and ciliates are dominant  
198 consumers of *E. huxleyi* and are frequently observed during *E. huxleyi* blooms<sup>48</sup>, short-  
199 term feeding experiments were conducted with the dinoflagellate *Gyrodinium dominans*  
200 and the ciliate *Strombidium* sp. as grazers. Like *O. marina*, *Strombidium* sp. consumed Tp  
201 DL-GFP prey faster than Tp GFP (~7-fold, Fig. 3a). In contrast, *G. dominans* grazed  
202 similarly on both prey types. Next, we assessed grazing by larger mesozooplankton (0.2–  
203 2 mm), on the transgenic diatoms. Cultured *Artemia salina* (brine shrimp) consumed Tp  
204 DL-GFP twice as fast as Tp GFP cells. Furthermore, wild calanoid copepods of the species  
205 *Pleuromamma indica* consumed Tp DL-GFP ~28 times more than the Tp GFP control (Fig.  
206 3a). Notably, none of the tested predators exhibited a negative grazing response toward Tp  
207 DL-GFP prey (fold-change  $< 1$ ). While DL-mediated herbivory may be species-specific, it  
208 is clearly not specific to *O. marina* alone, but shared by several important marine  
209 herbivores.

210 To further assess the ecological significance of DMS-mediated herbivory, we used mixed  
211 native microzooplankton assemblages from the Gulf of Aqaba in the northern Red Sea.  
212 These assemblages included a wide diversity of heterotrophic and mixotrophic species  
213 within the 5-200  $\mu\text{m}$  size range, such as tintinnid ciliates, dinoflagellates, nauplii and small  
214 copepods (Supplementary Fig. 8,9). Most natural cells  $< 5\mu\text{m}$  were excluded during net-  
215 tow harvesting. The native grazers were subsequently fed with Tp DL-GFP or Tp GFP prey  
216 cells for 24 h. The uptake of the transgenic diatom cells by the natural grazers was  
217 confirmed by microcopy and quantified as grazing rate ( $g, \text{day}^{-1}$ ) (Fig. 3b,c and  
218 Supplementary Fig. 10,11). Grazing rates in four independent experiments conducted  
219 during 2017-2020 were variable, perhaps due to changes in the taxonomic assortment of  
220 the grazer communities in each experimental flask. Nonetheless, in 3 out of 4 experiments,  
221 the native grazers removed the Tp DL-GFP prey cells significantly faster than the Tp GFP  
222 control. The highest average grazing rate was detected at February 2020, where Tp DL-  
223 GFP cells were removed on average ~10 times faster than Tp GFP control cells ( $0.22 \pm$   
224  $0.12 \text{ day}^{-1}$ , Fig. 3b). Overall, most of the cultured and wild grazers tested exhibited a varied  
225 degree of enhanced grazing on DMS-producing prey, indicating that DMS facilitates  
226 herbivory across a wide variety of zooplankton taxa representing different size and feeding  
227 strategies. To our knowledge, this is the first study to demonstrate that DL activity in algal  
228 prey cells is coupled to enhanced grazing activity by zooplankton.

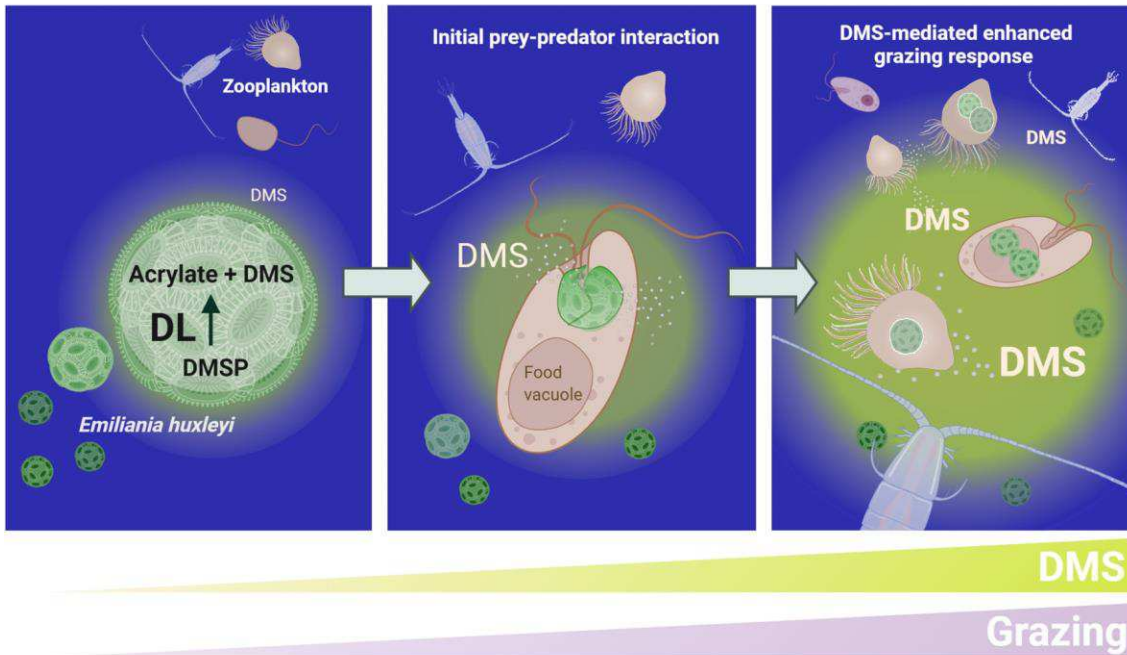


229

230 **Fig. 3. Induced DMS production in algal prey enhanced grazing by diverse zooplankton. a,**  
 231 **The grazing response of diverse zooplankton fed with Tp DL-GFP cells. Tp GFP cells were used**

232 as control prey. The fold change in grazing rate ( $g$ , as assessed by monitoring free prey cells using  
233 flow cytometry) on each prey type was calculated, where fold change  $> 1$  indicates faster grazing  
234 on Tp DL-GFP cells. Vertical lines represent the mean  $\pm$  SD;  $n = 3$  for *P. indica*; 4 for *A. salina*,  
235 *G. dominans* and *Strombidium* sp.; 6 for *O. marina*. n.s.- not significant,  $P > 0.897$ ;  $*P < 0.011$ ;  
236  $**P < 0.003$  (one-sample T-test). **b**, Grazing of Tp DL-GFP cells by natural microzooplankton  
237 from the Red Sea. Two prey types were offered to the microzooplankton assemblages: Tp GFP or  
238 Tp DL-GFP. Horizontal lines represent the mean;  $n=5-6$ .  $*P < 0.017$ ;  $**P < 0.005$  (Student's T-  
239 test). **c**, Variety of wild microzooplankton observed during grazing experiments shown in (b),  
240 including tintinnid ciliate (1), mixotrophic *Ceratium* dinoflagellates (2-3) and diverse copepods (4-  
241 6). Red represents the chlorophyll of ingested *T. pseudonana* cells added as prey (mixotrophic  
242 dinoflagellates also have endogenous chlorophyll).  
243

244 Our new results corroborate previous studies showing that DMS and DMSP can act as  
245 chemoattractant signals for marine protists (including *O. marina*) and copepods<sup>6,20,21,33</sup>.  
246 We therefore propose a new ecological role for the DL enzyme, mediated by its DMS  
247 product (and/or potentially acrylate) which acts as a pro-grazing signal and accelerating  
248 the removal of algal cells by their immediate protozoan predators. The response of marine  
249 protists to the algal-derived DMS signal is analogous to the phagocytic activity of immune  
250 cells in the mammals, which are attracted to damaged and apoptotic cells via secreted  
251 "eat-me" signals<sup>49</sup>. In light of our findings, DMS-mediated herbivory may have a  
252 significant impact on algal bloom dynamics of highly DMS-producing species like *E.*  
253 *huxleyi*. Since *E. huxleyi* strains can range in their DL activity over four order of magnitude  
254<sup>50-52</sup>, we hypothesize that grazing of high-DL strains can release DMS that acts as an  
255 appetizing signal, leading to enhanced grazing pressure imposed upon the entire blooming  
256 population (Fig. 4). Considering the constantly changing environmental conditions during  
257 bloom succession, and that late blooms are more prone to nutrient limitation and viral  
258 attack, DMS-mediated signaling may promote the removal of damaged, infected or aged  
259 algal populations by expediting a top-down grazing pressure.



260

261 **Fig. 4. The ecological impact of algal DMS on planktonic prey-predator interactions.** A  
 262 conceptual model describing DMS-mediated herbivory. Chemoattraction of zooplankton to leakage  
 263 of DMS from high DMS producing algae such of *E. huxleyi* cells may facilitate initial grazing  
 264 interaction (left panel). Upon dissociation of ingested cells during phagocytosis, the DL Alma1  
 265 degrades DMSP and releases more DMS into the water (middle panel). This microscale release of  
 266 DMS may accumulate to high concertation, which induces an increase in the overall grazing  
 267 pressure by diverse grazers on the entire phytoplankton population (right panel) and thus has wide  
 268 ecological implication in the marine environment.

269

270 Since the historical discovery of DMS from a seaweed about 85 years ago, the cellular  
271 function of this volatile, and of its generating enzyme, still remain elusive<sup>53</sup>. The unknown  
272 cellular role for the DL gene is intriguing in light of its high conservation among diverse  
273 phytoplankton species with great ecological success such as such as *E. huxleyi*, *Phaeocystis*  
274 and *Symbiodinium*<sup>7</sup>. While DMSP appears to serve as an osmolyte or antioxidant in several  
275 phytoplankton species<sup>15</sup>, the physiological benefit of DMSP catabolism by DL activity is  
276 still unknown. Yet, previous studies have indicated that DL activity acts as a grazing-  
277 activated chemical defense mechanism. The proposed defense role was based on grazing  
278 experiments on *E. huxleyi* strains displaying ~4 orders of magnitude range in the DL  
279 activity<sup>4,26,37,44</sup>. However, since the transcriptome of these *E. huxleyi* strains differs in  
280 expression of ~10,000 genes<sup>7,54</sup>, it is difficult to assign a specific role for a single trait as  
281 DL activity. Bulk addition of DMSP, but not of DMS or acrylate, reduced grazing rates of  
282 *E. huxleyi* cells by microzooplankton, suggesting a role in chemical defense<sup>5</sup>. However, it  
283 is questionable whether exogenous addition of DMS/P mimics spatiotemporal gradients in  
284 the media during prey-predator interaction. Indeed, based on our genetic and physiological  
285 approaches that enabled *in-vivo* modulation of DL activity, we show that DL activity  
286 enhanced grazing. Hence, the evolutionary retention of a DL gene comes with a marked  
287 cellular cost of prompting grazing by diverse herbivores. This conundrum indicates an  
288 essential role for DL activity in algal cells which is yet to be discovered.

289

290 At the ecological level, the response to DMS by zooplankton, and specifically  
291 microzooplankton as shown here, is akin to what has been previously described for higher  
292 predators such as fish, whales, birds and turtles. These top-predators utilize DMS as a  
293 foraging cue, to find ‘hot-spots’ of high biomass and high plankton concentrations<sup>22-24,55,56</sup>.  
294 Intriguingly, by facilitating trophic cascades, DMS may actually promote indirect defense  
295 mechanisms for the emitting phytoplankton at the population level. In the Southern Ocean,  
296 sea birds are highly sensitive to DMS emitted from *Phaeocystis* sp. blooms, track its source  
297 and feed mainly on krill, the main grazer of *Phaeocystis* sp. in this region<sup>22</sup>. In such  
298 tritrophic mutualism scenario, seabirds reduce grazing pressure on the phytoplankton.  
299 DMS was hypothesized to mediate pelagic tritrophic interactions in the plankton as well,  
300 where DMS-derived from phytoplankton-microzooplankton interaction triggers an indirect  
301 defense by attracting carnivorous mesozooplankton, which consume the microzooplankton  
302 and alleviate the grazing pressure imposed on the algal population<sup>57,58</sup>. This theory was  
303 supported by mathematical models<sup>59,60</sup> and evidence from coccolithophore and  
304 *Phaeocystis* blooms, where microzooplankton were found to be the main food source for  
305 mesozooplankton (copepods) rather than the coccolithophores directly<sup>61,62</sup>. Such copepods  
306 may be highly sensitive to DMS emitted during phytoplankton-microzooplankton grazing  
307 interaction<sup>21</sup>. In accord, we found that mesozooplankton (copepods and krill) fed with *O.*  
308 *marina* cells which were pre-treated with *E. huxleyi* or Tp DL-GFP prey, produced higher  
309 levels of fecal pellets. The mesozooplankton response was species-specific, and may

310 indicate enhanced copepod predation in the presence of grazing-derived DMS  
311 (Supplementary Table 3). The interlink between algal DMS and grazing at likely different  
312 trophic levels adds a new dimension to the complex trophic interactions established in  
313 oceanic ecosystems and particularly during algal blooms.

314

315 Overall, the sensing of DMS by marine biota from diverse size ranges and taxonomic  
316 groups<sup>6,63</sup> raises questions regarding the specificity of the DMS signal as a foraging cue,  
317 and suggests that DMS may serve as a global eat-me signal across trophic levels. The  
318 prevalence of algal-produced DMS and the ubiquity of DMS-mediated predator-prey  
319 interactions play fundamental roles in chemical communication among multiple trophic  
320 levels in the ocean.

321

322

## 323 **Methods**

324

### 325 **Culture maintenance**

326 Algal cultures (The diatom *Thalassiosira pseudonana* strain CCMP1335 and the  
327 coccolithophore *Emiliana huxleyi* CCMP373, CCMP374 and CCMP2090) were  
328 purchased from the National Center for Marine Algae and Microbiota (NCMA, East  
329 Boothbay, Maine). *Dunaliella tertiolecta* culture was kindly provided by Prof. Uri Pick,  
330 Weizmann Institute of Science. *Oxyrrhis marina* strain LB1974 was kindly provided by  
331 Dr. Matthew Johnson, Woods Hole Oceanographic Institute. *Strombidium sp.* and  
332 *Gyrodinium dominans* were isolated and kindly contributed by Dr. Albert Calbet, Institut  
333 de Ciències del Mar, CSIC. All cultures were grown at 18°C with 16 h : 8 h light:dark  
334 cycles, in light intensity of 100  $\mu\text{mol photons m}^{-2} \text{s}^{-1}$  for algal cultures and 50  $\mu\text{mol photons}$   
335  $\text{m}^{-2} \text{s}^{-1}$  for *O. marina*, supplied by cool white LED lights. Algae were diluted once weekly  
336 with autoclaved, 0.22  $\mu\text{m}$ -filtered seawater (FSW) supplemented with F/2 (and silica for  
337 diatoms)<sup>64</sup>. *O. marina* cells were fed twice weekly with *D. tertiolecta* and were transferred  
338 every 3 weeks to a new flask containing FSW supplemented with PenStrep antibiotic  
339 solution (Sigma).

340

### 341 **Genetic transformation of *T. pseudonana***

342 To overexpress the Alma1-GFP fusion protein in *T. pseudonana*, wild type cells were  
343 transformed using a biolistic particle delivery system fitted with 1350 psi rupture discs  
344 (BioRad). M10 tungsten particles (0.7  $\mu\text{m}$ ) were coated with 5  $\mu\text{g}$  of plasmid DNA in the  
345 presence of  $\text{CaCl}_2$  (2.5 M) and spermidine, according to the manufacturer's instructions.  
346 The plasmid encodes for nourseothricin resistance and Alma or Alma-GFP fusion protein.  
347 Approximately  $1 \times 10^6$  cells were spread on a plate containing solid medium (1.5% Bacto  
348 agar in FSW + F/2) a few hours before bombardment. Bombarded cells were recovered in  
349 F/2 media + silica, and incubated at 18°C under constant light overnight. The culture was

350 then plated onto solid medium containing 100  $\mu\text{g mL}^{-1}$  nourseothricin. Plates were  
351 incubated for 10 days and resistant colonies were re-streaked onto fresh solid medium  
352 containing nourseothricin. The colonies obtained were then screened for GFP fluorescence  
353 and DL activity.  
354

### 355 **Measurements of cellular DMSP, DMS emission and DMSP lyase activity**

356 For determination of cellular DMSP concentration, cultures (~3 ml) were acidified with  
357 1.5 % HCl and stored at 4°C for >24 hours<sup>17</sup>. Samples were diluted (1:100) in DDW, and  
358 DMSP was lysed to DMS by adding NaOH to a final concentration of 0.45 M. Glycine  
359 buffer (pH 3, final con. 0.8 M) was added in order to neutralize the solution (pH 8 to 9).  
360 Samples were then measured for DMS concentration in sealed glass vials, using Eclipse  
361 4660 Purge-and-Trap Sample Concentrator system equipped with Autosampler (OI  
362 Analytical). Separation and detection were done using gas chromatography-flame  
363 photometric detector (GC-FPD, HP 5890) equipped with RT-XL sulfur column (Restek).  
364 DMS emission *in-vivo* was quantified in the culture media (filtered through GF/F filters,  
365 Whatman) or directly in the culture over time, in sealed glass vials (40 mL). The DMS  
366 measurement itself was conducted as described for the DMSP analysis. DMSP lyase activity  
367 (*in-vitro*) was estimated as DMS release and measured as previously described<sup>7</sup>. Cells  
368 were harvested by centrifugation. Cell pellets were resuspended in lysis buffer (Tris 100  
369 mM pH 8.0, NaCl 100 mM, DTT 1 mM, Triton 100x 0.02%, Benzonase 250 units) and  
370 sonicated. Crude lysates were incubated with 10 mM DMSP while shaking for 10 min at  
371 30°C. Reactions were terminated by 1000-fold dilution into sealed glass vials containing  
372 30 ml of distilled water. The vials were kept on ice in the dark until the DMS measurement,  
373 conducted as described for the DMSP analysis. All measurements were calibrated against  
374 a standard curve of DMS, ranging from 5 to 300 nM (Sigma-Aldrich).  
375

### 376 **Western-blot analysis**

377 For detection of the Alma1 protein expression, cells were harvested at exponential growth  
378 phase by centrifugation (10,000  $\times g$ , 15 min, 4°C) and plunged into liquid nitrogen. Cell  
379 pellets were then resuspended in lysis buffer and bath-sonicated (5.5 s sonication following  
380 by 10 s rest, x 5 cycles). Cell lysates and recombinant Alma1, used as a positive control<sup>7</sup>,  
381 were separated on an Any kD SDS-PAGE (Bio-Rad). For western-blot analysis, we used a  
382 primary rabbit polyclonal antibody raised by immunization against the recombinant Alma1  
383 protein<sup>7</sup> and a secondary horseradish peroxidase-conjugated anti-rabbit antibody (Sigma-  
384 Aldrich). The antibodies were diluted in Tris-buffered saline containing 0.1% Tween-20  
385 and 5% skim-milk powder. ECL-Prime reagent (GE Healthcare) was used for detection.  
386

### 387 **Scanning electron microscopy of *T. pseudonana* cells**

388 For morphological analysis of *T. pseudonana* cells, samples were collected during  
389 exponential growth phase. Samples (1 mL) were blotted at room temperature on Nuclepore

390 track-etched polycarbonate membranes (Whatman), coated with 5 nm of Iridium for  
391 improved conductance, and imaged with a Sigma 500 SEM (Zeiss) using the InLens  
392 detector.

393

#### 394 **Grazing assays with *O. marina*, *Gyrodinium dominans* and *Strombidium* sp.**

395 Grazing assays were conducted mainly with *O. marina* as predator and *E. huxleyi* or *T.*  
396 *pseudonana* as prey. Prior to the assay, microzooplankton were starved for 3 days to clear  
397 their digestive vacuole from their routine prey, *D. tertiolecta*. Prey cells were added to the  
398 grazer culture to reach a final prey:grazer ratio of 3:1 or 10:1 ( $1-30 \times 10^4$  prey cells  $\text{mL}^{-1}$ ).  
399 Grazer concentration was  $3 \times 10^3$  cells  $\text{mL}^{-1}$ . Grazing assays with *O. marina* were  
400 conducted for 0.5-24 h, as designated in each graph. For *Gyrodinium dominans* and  
401 *Strombidium* sp., grazing assay was conducted for 3 h.

402 When using Br-DMSP<sup>8</sup>, the inhibitor was added to the *E. huxleyi* culture 2 h prior to  
403 grazing interaction. The inhibitor was diluted with MeOH and added in a final  
404 concentration of 0.2  $\mu\text{M}$ , which was chosen based on toxicity assays (Supplementary Fig.  
405 1). The same volume of MeOH was used as control. The inhibitor's toxicity for *O. marina*  
406 cells was tested by using SYTOX Green (Invitrogen) staining to detect compromised cell  
407 membranes. Samples were stained with a final concentration of 1  $\mu\text{M}$  SYTOX, incubated  
408 in the dark for 30 min and analyzed by an Eclipse flow cytometer, as described below (ex:  
409 488 nm and em: 500–550 nm). An unstained sample was used to eliminate the background  
410 signal.

411

#### 412 **Determination of grazing and ingestion rates**

413 For grazing rate (g) and ingestion rate (IR) analyses, prey and grazer were incubated in a  
414 24 well plate. Prey cells were also added to FSW as a growth control. Each group included  
415 4-6 biological replicates. The plate was placed in the flow cytometer autosampler, where  
416 each well was sampled every 30 min to quantify the algal cells, for a total period of 2-4  
417 hours. The flow cytometer, Eclipse iCyt (Sony Biotechnology Inc., Champaign, IL, USA),  
418 was equipped with 488 nm solid state air cooled laser, with 25 mW on the flow cell and  
419 with standard filter set-up. Algal cells were identified by plotting the chlorophyll  
420 fluorescence (ex: 488 nm and em: 663-737 nm) against side scatter. At least 2,500 cells  
421 were collected in each sample. Grazer cells were counted manually. The algal specific  
422 growth rate ( $\mu$ ) was calculated for the control and grazing treatments. g and IR were  
423 calculated based on  $\mu$  and normalized per grazer, as described by Frost<sup>65</sup>.

424

#### 425 ***O. marina* vacuole content (VC) analysis**

426 Manual quantification of ingested prey was adapted from previous studies<sup>26</sup>. Incubation  
427 of prey and predator were conducted in 50 mL culture flasks. Sub-samples were fixed with  
428 1% PFA at two time points (0.5, 3h) for *E. huxleyi* or during a time course for *T.*  
429 *pseudonana* (8, 17, 30, 45 and 60 min) prey. Fixed cells were gently transferred into an

430 Utermoehl sedimentation system (Aquatic Research Instruments, USA) and collected onto  
431 a microscope slide for 24 hours. Ingested prey items were counted by using an IX71S1F-  
432 3-5 inverted Olympus microscope (Tokyo, Japan), equipped with an EXi Blue camera (Q  
433 Imaging, Surrey, BC, Canada). 100 grazer cells were observed per sample. The average  
434 prey content was calculated for each sample.

435

#### 436 ***O. marina* growth curve**

437 To quantify the effect of DMS-producing prey on grazer growth, *O. marina* culture was  
438 divided to three dietary treatments: starvation, *T. pseudonana* wild type and Tp DL-GFP  
439 prey. Each treatment contained four 50 mL small flasks, which represent biological  
440 replicates. Prey cells were supplied daily and added to a final concentration of  $3 \times 10^4$  cells  
441  $\text{mL}^{-1}$ . The flasks were mounted onto a rotating plankton wheel and incubated with the  
442 growth condition indicated above. Daily samples for grazer cell count were fixed with 10%  
443 Lugol (Sigma-Aldrich) in a 24-well plate. *O. marina* cells were counted by using an  
444 IX71S1F-3-5 inverted Olympus microscope (described above). A total of 140-1000 cells  
445 were counted per sample.

446

#### 447 **Grazing assays with natural microzooplankton assemblages**

448 In order to assess grazing on transgenic diatoms by natural microzooplankton, experiments  
449 were conducted during 2017-2020 at The Inter-University Institute for Marine Sciences  
450 (IUI) in Eilat, Israel. Surface water was collected from the pier area ( $29^\circ 50' \text{ N}$ ,  $34^\circ 91' \text{ E}$ )  
451 by using a concentrating plankton net ( $5 \mu\text{m}$ ). Sampled water (4 L) was then gently sieved  
452 through a  $200 \mu\text{m}$  mesh in order to obtain the 5-200  $\mu\text{m}$  microzooplankton community  
453 fraction (used for the “grazing” treatment). Seawater was also filtered through  $0.22 \mu\text{m}$   
454 filter to remove all cells (used for the “growth” treatment). Each water fraction (5-200  $\mu\text{m}$   
455 and  $<0.22 \mu\text{m}$ ) was divided to 300-830 mL polycarbonate flasks. Diatom cultures (Tp GFP  
456 or Tp DL-GFP) were added to the flasks ( $3 \times 10^4 \text{ cell mL}^{-1}$ ) at  $T_0$ , including 5-6 biological  
457 replicates. Incubation flasks were placed in a shaded water-table with ambient water  
458 temperature ( $22\text{-}23^\circ\text{C}$ ) for 24 h. In 2020, the incubation flasks were mounted onto a rotating  
459 wheel (0.3 rpm) and placed in the dark at  $22^\circ\text{C}$  for 24 h. Samples for cell count were taken  
460 at  $T_0$  and after 24 h, using FCM as describe above.

461 Grazing rate was calculated as previously described<sup>66</sup>. First, the growth rate was calculated  
462 for each flask as:  $\mu = (\ln C_{24} - \ln C_0) / (T_{24} - T_0)$ , where  $C_{24}$  and  $C_0$  are the concentration of  
463 cells at  $T_{24}$  and  $T_0$ , respectively. Then, the grazing coefficient  $g$  was calculated by:  $g =$   
464  $\mu_{\text{growth}} - \mu_{\text{grazing}}$ , using the average  $\mu$  for the growth treatment.

#### 465 **Grazing assays with *Artemia salina* and *Pleuromamma indica***

466 In order to assess grazing on DMS-producing prey by *Artemia salina*, grazing experiments  
467 were conducted with 15 days old females which were starved for 3 days. Four individuals  
468 were washed with FSW and carefully transferred using a pipette to 50 mL flasks containing  
469 FSW or transgenic *T. pseudonana* cultures (Tp DL-GFP or Tp GFP). Initial prey

470 concentration was  $1 \times 10^5$  cell  $\text{mL}^{-1}$ . Algal cells were counted by FCM at  $T_0$  and 1-3 h and  
471  $g$  was calculated as in Frost<sup>65</sup>. Grazing experiments with *Pleuromamma indica* were  
472 conducted with wild animals collected at the northern Gulf of Aqaba, Red Sea (Station A,  
473  $29^\circ 28' \text{ N}$ ,  $34^\circ 56' \text{ E}$ ) by using 300  $\mu\text{m}$  mesh nets. Populations *P. indica* were carefully  
474 isolated from the heterogeneous assemblages. Groups of 10 individuals were transferred to  
475 petri dishes with FSW for 6-10 hours to allow evacuation of their gut content. At  $T_0$ , the  
476 animals were transferred to incubation flasks (300 mL, 10 per flask), supplemented with  
477 FSW or transgenic *T. pseudonana* cultures (Tp DL-GFP or Tp GFP,  $3 \times 10^4$  cell  $\text{mL}^{-1}$ ). Algal  
478 cells were counted by FCM at  $T_0$  and 48 h and  $g$  was calculated as in Frost<sup>65</sup>.  
479

### 480 **Mesozooplankton tritrophic grazing experiments**

481 In order to assess grazing and defecation by mesozooplankton in a tritrophic setup, samples  
482 were collected during 2019-2020 at the northern Gulf of Aqaba, Red Sea (Station A,  $29^\circ$   
483  $28' \text{ N}$ ,  $34^\circ 56' \text{ E}$ ) by using 300  $\mu\text{m}$  mesh nets. Populations of *Euphausia diomedea*,  
484 *Rhincalanus nasutus* and *Pleuromamma indica* were carefully isolated from the  
485 heterogeneous assemblages. The three species were used in separate experiments, where  
486 their gut content and FP production were quantified in response to different dietary  
487 treatments. Groups of 10-12 individuals were transferred to petri dishes with FSW for 6-  
488 10 hours to allow evacuation of their gut content. At  $T_0$ , the animals were transferred to  
489 incubation flasks (300 mL), supplemented with FSW or *O. marina* and phytoplankton  
490 cultures. *O. marina* was incubated with phytoplankton ( $3 \times 10^3$  cells  $\text{mL}^{-1}$  and  $3 \times 10^4$  cells  
491  $\text{mL}^{-1}$ , respectively) for a few hours prior to the addition of mesozooplankton, in order for  
492 *O. marina* to feed and allow the accumulation of grazing-derived chemical cues. Incubation  
493 flasks were mounted onto a rotating wheel (0.3 rpm) and incubated in the dark at  $22^\circ\text{C}$  for  
494 48 h. At  $T_{48}$ , the animals were collected from the incubation flasks, washed with FSW and  
495 flash-frozen in liquid nitrogen (all animals from the same flask were grouped into a single  
496 tube prior to freezing). The specific ingestion of *O. marina* cells was confirmed by  
497 detecting an *O. marina* DNA sequence within the copepod gut. DNA was extracted from  
498 whole copepods by classical phenol-chloroform extraction, and then cleaned by AMPure  
499 XP beads (Beckman Coulter). Primers for quantitative PCR were designed by Primer3 and  
500 Amplify4 (William Engels, University of Wisconsin 2015) to amplify the mitochondrial  
501 *cob-cox3* gene, which is unique to *O. marina*<sup>67,68</sup>. Forward primer: 5'  
502 TCATGCTTTTATCTTTCTATCCA 3'; reverse primer:  
503 5'AGCTAAGAATAAAGTAGAAGGAGA 3'. For qPCR, Platinum SYBR Green qPCR  
504 SuperMix-UDG with ROX was used as described by the manufacturer (Invitrogen).  
505 Reactions were performed on Step-One Plus real-time PCR System (Applied Biosystems)  
506 as follows:  $50^\circ\text{C}$  for 2 min,  $95^\circ\text{C}$  for 2 min, 40 cycles of  $95^\circ\text{C}$  for 15 s,  $60^\circ\text{C}$  for 30 s.

507

## 508 **Statistical analysis**

509 Group comparisons were conducted with Student's t-test (for two groups) or ANOVA (for  
510 more than two groups) followed by Tukey's or Dunnett's post-hoc tests. Experiments with  
511 repeated measures per vial were tested with mixed effects models, treating vial as a random  
512 factor. A generalized linear model with Poisson distribution was used when analyzing  
513 discrete counts. All analyses were conducted in R, v. 4.0.2. GLMs were done using the  
514 package "lmerTest", v. 3.1-2.

515

516 Illustrations were created with BioRender.com.

517 Graphs were created with GraphPad Prism.

518

519

## 520 **Acknowledgments**

521 We thank Inbal Nussbaum and Alon Spierer for assisting in laboratory experiments; Yaara  
522 Finkel for helping in genetic transformation of *T. pseudonana*; Diana Meltzer for  
523 synthesizing Br-DMSP used in grazing experiments; Emanuel M. Avrahami for  
524 conducting scanning electron microscopy analysis for *T. pseudonana* cells; Yoav  
525 Avrahami for helping with field sampling and flow cytometry; Flora Vincent and  
526 Constanze Kuhlisch for their constructive feedback on the manuscript. We gratefully  
527 acknowledge financial support from the Israeli Science Foundation (ISF) (grant #712233)  
528 awarded to A.V. All data are available in the supplementary materials.

529 Author contributions: A.S. and A.V. conceptualized the research questions and hypothesis,  
530 designed the experiments and wrote the manuscript. A.S. performed all the experiments  
531 and analyzed the data. U.A., M.J.F. and D.S.T helped in establishing the experimental  
532 system, developing the experimental tools and contributed in scientific discussions. D.S.  
533 conducted genetic transformation of *T. pseudonana*. A.S. and V.F. designed and conducted  
534 mesozooplankton grazing experiments. S.B.-D. performed bioinformatics analysis. R.R.  
535 performed statistical analysis.

536

## 537 **References**

- 538 1 Simó, R. Production of atmospheric sulfur by oceanic plankton: biogeochemical,  
539 ecological and evolutionary links. *Trends. Ecol. Evol.* **16**, 287-294, doi:10.1016/S0169-  
540 5347(01)02152-8 (2001).
- 541 2 Charlson, R. J., Lovelock, J. E., Andreae, M. O. & Warren, S. G. Oceanic phytoplankton,  
542 atmospheric sulphur, cloud albedo and climate. *Nature* **326**, 655-661 (1987).
- 543 3 Wang, S., Maltrud, M. E., Burrows, S. M., Elliott, S. M. & Cameron-Smith, P. Impacts of  
544 shifts in phytoplankton community on clouds and climate via the sulfur cycle. *Global*  
545 *Biogeochem. Cy.* **32**, 1005-1026, doi:<https://doi.org/10.1029/2017GB005862> (2018).

- 546 4 Wolfe, G. V., Steinke, M. & Kirst, G. O. Grazing-activated chemical defence in a  
547 unicellular marine alga. *Nature* **387**, 894-897 (1997).
- 548 5 Strom, S., Wolfe, G., Slajer, A., Lambert, S. & Clough, J. Chemical defense in the  
549 microplankton II: Inhibition of protist feeding by  $\beta$ -dimethylsulfoniopropionate (DMSP).  
550 *Limnol. Oceanogr.* **48**, 230-237, doi:10.4319/lo.2003.48.1.0230 (2003).
- 551 6 Seymour, J., Simó, R., Ahmed, T. & Stocker, R. Chemoattraction to  
552 dimethylsulfoniopropionate throughout the marine microbial food web. *Science (New*  
553 *York, N.Y.)* **329**, 342-345 (2010).
- 554 7 Alcolombri, U. *et al.* Identification of the algal dimethyl sulfide-releasing enzyme: A  
555 missing link in the marine sulfur cycle. *Science (New York, N.Y.)* **348**, 1466-1469,  
556 doi:10.1126/science.aab1586 (2015).
- 557 8 Alcolombri, U., Lei, L., Meltzer, D., Vardi, A. & Tawfik, D. S. Assigning the algal source  
558 of dimethylsulfide using a selective lyase inhibitor. *ACS Chem. Biol.* **12**, 41-46,  
559 doi:10.1021/acscchembio.6b00844 (2017).
- 560 9 Kettle, A. J. & Andreae, M. Flux of dimethylsulfide from the oceans: A comparison of  
561 updated data sets and flux models. *J. Geophys. Res.* **105**, doi:10.1029/2000JD900252  
562 (2000).
- 563 10 Carpenter, L. J., Archer, S. D. & Beale, R. Ocean-atmosphere trace gas exchange. *Chem.*  
564 *Soc. Rev.* **41**, 6473-6506, doi:10.1039/C2CS35121H (2012).
- 565 11 Franklin, D. J. *et al.* Identification of senescence and death in *Emiliana huxleyi* and  
566 *Thalassiosira pseudonana*: Cell staining, chlorophyll alterations, and  
567 dimethylsulfoniopropionate (DMSP) metabolism. *Limnol. Oceanogr.* **57**, 305-317,  
568 doi:10.4319/lo.2012.57.1.0305 (2012).
- 569 12 Keller, M. D. Dimethyl sulfide production and marine phytoplankton: the importance of  
570 species composition and cell size. *Biol. Oceanogr.* **6**, 375-382,  
571 doi:10.1080/01965581.1988.10749540 (1989).
- 572 13 Curson, A. R. J. *et al.* DSYB catalyses the key step of dimethylsulfoniopropionate  
573 biosynthesis in many phytoplankton. *Nat. Microbiol.* **3**, 430-439, doi:10.1038/s41564-018-  
574 0119-5 (2018).
- 575 14 Sunda, W., Kieber, D. J., Kiene, R. P. & Huntsman, S. An antioxidant function for DMSP  
576 and DMS in marine algae. *Nature* **418**, 317-320,  
577 doi:http://www.nature.com/nature/journal/v418/n6895/supinfo/nature00851\_S1.html  
578 (2002).
- 579 15 Kirst, G. O. in *Biological and environmental chemistry of DMSP and related sulfonium*  
580 *compounds* (eds Ronald P. Kiene, Pieter T. Visscher, Maureen D. Keller, & Gunter O.  
581 Kirst) 121-129 (Springer US, 1996).
- 582 16 Darroch, L. *et al.* Effect of short-term light and UV stress on DMSP, DMS, and DMSP  
583 lyase activity in *Emiliana huxleyi*. *Aquat. Microb. Ecol.* **74**, 173-185,  
584 doi:10.3354/ame01735 (2015).
- 585 17 Barak-Gavish, N. *et al.* Bacterial virulence against an oceanic bloom-forming  
586 phytoplankter is mediated by algal DMSP. *Sci. Adv.* **4**, eaau5716,  
587 doi:10.1126/sciadv.aau5716 (2018).
- 588 18 Amin, S. A. *et al.* Interaction and signalling between a cosmopolitan phytoplankton and  
589 associated bacteria. *Nature* **522**, 98-101, doi:10.1038/nature14488 (2015).
- 590 19 Garcés, E., Alacid, E., Reñé, A., Petrou, K. & Simó, R. Host-released dimethylsulphide  
591 activates the dinoflagellate parasitoid *Parvilucifera sinerae*. *ISME J.* **7**, 1065-1068,  
592 doi:10.1038/ismej.2012.173 (2013).
- 593 20 Steinke, M., Stefels, J. & Stams, E. Dimethyl sulfide triggers search behavior in  
594 copepods. *Limnol. Oceanogr.* **51**, 1925-1930, doi:10.4319/lo.2006.51.4.1925 (2006).

- 595 21 Breckels, M., Bode, N., Codling, E. & Steinke, M. Effect of grazing-mediated dimethyl  
596 sulfide (DMS) production on the swimming behavior of the copepod *Calanus*  
597 *helgolandicus*. *Mar. Drugs* **11**, 2486 (2013).
- 598 22 Savoca, M. S. & Nevitt, G. A. Evidence that dimethyl sulfide facilitates a tritrophic  
599 mutualism between marine primary producers and top predators. *Proc. Natl. Acad. Sci.*  
600 *U.S.A.* **111**, 4157-4161, doi:10.1073/pnas.1317120111 (2014).
- 601 23 Bouchard, B. *et al.* Behavioural responses of humpback whales to food-related chemical  
602 stimuli. *PLOS ONE* **14**, e0212515, doi:10.1371/journal.pone.0212515 (2019).
- 603 24 Endres, C. S. & Lohmann, K. J. Perception of dimethyl sulfide (DMS) by loggerhead sea  
604 turtles: a possible mechanism for locating high-productivity oceanic regions for foraging.  
605 *J. Exp. Biol.* **215**, 3535-3538, doi:10.1242/jeb.073221 (2012).
- 606 25 Simó, R. *et al.* The quantitative role of microzooplankton grazing in dimethylsulfide  
607 (DMS) production in the NW Mediterranean. *Biogeochemistry*, doi:10.1007/s10533-018-  
608 0506-2 (2018).
- 609 26 Strom, S. *et al.* Chemical defense in the microplankton I: Feeding and growth rates of  
610 heterotrophic protists on the DMS-producing phytoplankter *Emiliana huxleyi*. *Limnol*  
611 *Oceanogr.* **48**, 217-229, doi:10.4319/lo.2003.48.1.0217 (2003).
- 612 27 Lehahn, Y. *et al.* Decoupling physical from biological processes to assess the impact of  
613 viruses on a mesoscale algal bloom. *Curr. Biol.* **24**, 2041-2046,  
614 doi:10.1016/j.cub.2014.07.046 (2014).
- 615 28 Laber, C. P. *et al.* Coccolithovirus facilitation of carbon export in the North Atlantic. *Nat.*  
616 *Microbiol.* **3**, 537-547, doi:10.1038/s41564-018-0128-4 (2018).
- 617 29 Burkill, P. *et al.* Dimethyl sulphide biogeochemistry within a coccolithophore bloom  
618 (DISCO): An overview. *DEEP-SEA RES PT II* **49**, 2863-2885, doi:10.1016/S0967-  
619 0645(02)00061-9 (2002).
- 620 30 Calbet, A. & Landry, M. R. Phytoplankton growth, microzooplankton grazing, and carbon  
621 cycling in marine systems. *Limnol. Oceanogr.* **49**, 51-57, doi:10.4319/lo.2004.49.1.0051  
622 (2004).
- 623 31 Schmoker, C., Hernández-León, S. & Calbet, A. Microzooplankton grazing in the oceans:  
624 impacts, data variability, knowledge gaps and future directions. *J. Plankton. Res.* **35**, 691-  
625 706, doi:10.1093/plankt/fbt023 (2013).
- 626 32 Landry, M. R. & Calbet, A. Microzooplankton production in the oceans. *ICES J. Mar. Sci.*  
627 **61**, 501-507, doi:10.1016/j.icesjms.2004.03.011 (2004).
- 628 33 Breckels, M. N., Roberts, E. C., Archer, S. D., Malin, G. & Steinke, M. The role of  
629 dissolved infochemicals in mediating predator-prey interactions in the heterotrophic  
630 dinoflagellate *Oxyrrhis marina*. *J. Plankton. Res.* **33**, 629-639, doi:10.1093/plankt/fbq114  
631 (2010).
- 632 34 Raina, J. B. *et al.* Subcellular tracking reveals the location of dimethylsulfoniopropionate  
633 in microalgae and visualises its uptake by marine bacteria. *eLife* **6**, e23008,  
634 doi:10.7554/eLife.23008 (2017).
- 635 35 Evans, C., Kadner, S. V. & Darroch, L. J. The relative significance of viral lysis and  
636 microzooplankton grazing as pathways of dimethylsulfoniopropionate (DMSP) cleavage:  
637 An *Emiliana huxleyi* culture study. *Limnol. Oceanogr.* **52**, 1036-1045 (2007).
- 638 36 van Rijssel, M. & Gieskes, W. W. C. Temperature, light, and the  
639 dimethylsulfoniopropionate (DMSP) content of *Emiliana huxleyi* (Prymnesiophyceae). *J.*  
640 *Sea Res.* **48**, 17-27, doi:https://doi.org/10.1016/S1385-1101(02)00134-X (2002).
- 641 37 Wolfe, G. V. & Steinke, M. Grazing-activated production of dimethyl sulfide (DMS) by  
642 two clones of *Emiliana huxleyi*. *Limnol. Oceanogr.* **41**, 1151-1160,  
643 doi:10.4319/lo.1996.41.6.1151 (1996).

- 644 38 Daly, K. L. & DiTullio, G. R. in *Biological and environmental chemistry of DMSP and*  
645 *related sulfonium compounds* (eds Ronald P. Kiene, Pieter T. Visscher, Maureen D.  
646 Keller, & Gunter O. Kirst) 223-238 (Springer US, 1996).
- 647 39 Poulsen, N., Chesley, P. M. & Kröger, N. Molecular genetic manipulation of the diatom  
648 *Thalassiosira pseudonana* (bacillariophyceae). *J. Phycol.* **42**, 1059-1065,  
649 doi:10.1111/j.1529-8817.2006.00269.x (2006).
- 650 40 Saade, A. & Bowler, C. Molecular tools for discovering the secrets of diatoms. *BioScience*  
651 **59**, 757-765, doi:10.1525/bio.2009.59.9.7 (2009).
- 652 41 Armbrust, E. V. *et al.* The genome of the diatom *Thalassiosira pseudonana*: ecology,  
653 evolution, and metabolism. *Science (New York, N.Y.)* **306**, 79-86,  
654 doi:10.1126/science.1101156 (2004).
- 655 42 Malviya, S. *et al.* Insights into global diatom distribution and diversity in the world's ocean.  
656 *Proc. Natl. Acad. Sci. U.S.A.* **113**, E1516-1525, doi:10.1073/pnas.1509523113 (2016).
- 657 43 Kettles, N. L., Kopriva, S. & Malin, G. Insights into the regulation of DMSP synthesis in  
658 the diatom *Thalassiosira pseudonana* through APR activity, proteomics and gene  
659 expression analyses on cells acclimating to changes in salinity, light and nitrogen. *PLOS*  
660 *ONE* **9**, e94795, doi:10.1371/journal.pone.0094795 (2014).
- 661 44 Steinke, M., Wolfe, G. V. & Kirst, G. O. Partial characterisation of  
662 dimethylsulfoniopropionate (DMSP) lyase isozymes in 6 strains of *Emiliania huxleyi*. *Mar.*  
663 *Ecol.* **175**, 215-225 (1998).
- 664 45 Lana, A. *et al.* An updated climatology of surface dimethylsulfide concentrations and  
665 emission fluxes in the global ocean. *Global Biogeochem. Cyc.* **25**,  
666 doi:10.1029/2010gb003850 (2011).
- 667 46 Royer, S. J. *et al.* A high-resolution time-depth view of dimethylsulphide cycling in the  
668 surface sea. *Sci. Rep.* **6**, 32325, doi:10.1038/srep32325 (2016).
- 669 47 Saló, V., Simó, R., Vila-Costa, M. & Calbet, A. Sulfur assimilation by *Oxyrrhis marina*  
670 feeding on a 35S-DMSP-labelled prey. *Environ. Microbiol.* **11**, 3063-3072,  
671 doi:10.1111/j.1462-2920.2009.02011.x (2009).
- 672 48 Olson, M. B. & Strom, S. L. Phytoplankton growth, microzooplankton herbivory and  
673 community structure in the southeast Bering Sea: insight into the formation and temporal  
674 persistence of an *Emiliania huxleyi* bloom. *DEEP-SEA RES PT II* **49**, 5969-5990,  
675 doi:https://doi.org/10.1016/S0967-0645(02)00329-6 (2002).
- 676 49 Li, W. Eat-me signals: keys to molecular phagocyte biology and "appetite" control. *J. Cell*  
677 *Physiol.* **227**, 1291-1297, doi:10.1002/jcp.22815 (2012).
- 678 50 Read, B. A. *et al.* Pan genome of the phytoplankton *Emiliania* underpins its global  
679 distribution. *Nature* **499**, 209-213, doi:10.1038/nature12221 (2013).
- 680 51 Martínez, J. M., Schroeder, D. C. & Wilson, W. H. Dynamics and genotypic composition  
681 of *Emiliania huxleyi* and their co-occurring viruses during a coccolithophore bloom in the  
682 North Sea. *FEMS Microbiol. Ecol.* **81**, 315-323, doi:10.1111/j.1574-6941.2012.01349.x  
683 (2012).
- 684 52 Krueger-Hadfield, S. A. *et al.* Genotyping an *Emiliania huxleyi* (prymnesiophyceae) bloom  
685 event in the North Sea reveals evidence of asexual reproduction. *Biogeosciences* **11**, 5215-  
686 5234, doi:10.5194/bg-11-5215-2014 (2014).
- 687 53 Haas, P. The liberation of methyl sulphide by seaweed. *Biochem. J.* **29**, 1297-1299,  
688 doi:10.1042/bj0291297 (1935).
- 689 54 von Dassow, P. *et al.* Transcriptome analysis of functional differentiation between haploid  
690 and diploid cells of *Emiliania huxleyi*, a globally significant photosynthetic calcifying cell.  
691 *Genome Biol.* **10**, R114, doi:10.1186/gb-2009-10-10-r114 (2009).
- 692 55 Foretich, M. A., Paris, C. B., Grosell, M., Stieglitz, J. D. & Benetti, D. D. Dimethyl sulfide  
693 is a chemical attractant for reef fish larvae. *Sci. Rep.* **7**, 2498, doi:10.1038/s41598-017-  
694 02675-3 (2017).

695 56 Savoca, M. S. Chemoattraction to dimethyl sulfide links the sulfur, iron, and carbon cycles  
696 in high-latitude oceans. *Biogeochemistry* **138**, 1-21, doi:10.1007/s10533-018-0433-2  
697 (2018).

698 57 Steinke, M., Malin, G. & Liss, P. Trophic interactions in the sea: An ecological role for  
699 climate relevant volatiles? *J. Phycol.* **38**, 630-638, doi:10.1046/j.1529-8817.2002.02057.x  
700 (2002).

701 58 Pohnert, G., Steinke, M. & Tollrian, R. Chemical cues, defence metabolites and the shaping  
702 of pelagic interspecific interactions. *Trends Ecol. Evol.* **22**, 198-204,  
703 doi:10.1016/j.tree.2007.01.005 (2007).

704 59 Lewis, N. *et al.* Grazing-induced production of DMS can stabilize food-web dynamics and  
705 promote the formation of phytoplankton blooms in a multitrophic plankton model.  
706 *Biogeochemistry* **110**, 303-313, doi:10.1007/s10533-011-9649-0 (2012).

707 60 Lewis, N. D. Role of infochemical mediated zooplankton grazing in a phytoplankton  
708 competition model. *Ecol. complex.* **16**, pp. 41-50-2013 v.2016,  
709 doi:10.1016/j.ecocom.2012.10.003 (2013).

710 61 Hansen, F. C., Reckermann, M., Breteler, W. C. M. K. & Riegman, R. Phaeocystis  
711 blooming enhanced by copepod predation on protozoa: evidence from incubation  
712 experiments. *Mar. Ecol. Prog. Ser.* **102**, 51-57 (1993).

713 62 Levasseur, M. *et al.* Production of DMSP and DMS during a mesocosm study of an  
714 *Emiliania huxleyi* bloom: Influence of bacteria and *Calanus finmarchicus* grazing. *Mar.*  
715 *Biol.* **126**, 609-618, doi:10.1007/BF00351328 (1996).

716 63 Buchan, A., LeClerc, G. R., Gulvik, C. A. & González, J. M. Master recyclers: features and  
717 functions of bacteria associated with phytoplankton blooms. *Nat. Rev. Microbiol.* **12**, 686,  
718 doi:10.1038/nrmicro3326 (2014).

719 64 Guillard, R. R. L. & Ryther, J. H. Studies of marine planktonic diatoms. I. *Cyclotella nana*  
720 Hustedt, and *Detonula confervacea* (Cleve) Gran. *Can. J. Microbiol.* **8**, 229-239,  
721 doi:10.1139/m62-029 (1962).

722 65 Frost, B. W. Effects of size and concentration of food particles on the feeding behavior of  
723 the marine planktonic copepod *Calanus Pacificus*. *Limnol. Oceanogr.* **17**, 805-815,  
724 doi:10.4319/lo.1972.17.6.0805 (1972).

725 66 Johnson, M. D., Michelle, R. & Stoecker, D. K. Microzooplankton grazing on  
726 *Prorocentrum minimum* and *Karlodinium micrum* in Chesapeake Bay. *Limnol. Oceanogr.*  
727 **48**, 238-248, doi:10.4319/lo.2003.48.1.0238 (2003).

728 67 Slamovits, C. H., Saldarriaga, J. F., Larocque, A. & Keeling, P. J. The highly reduced and  
729 fragmented mitochondrial genome of the early-branching dinoflagellate *Oxyrrhis marina*  
730 shares characteristics with both apicomplexan and dinoflagellate mitochondrial genomes.  
731 *J. Mol. Biol.* **372**, doi:10.1016/j.jmb.2007.06.085 (2007).

732 68 Untergasser, A. *et al.* Primer3Plus, an enhanced web interface to Primer3. *Nucleic acids*  
733 *Res.* **35**, W71-74, doi:10.1093/nar/gkm306 (2007).

# Figures

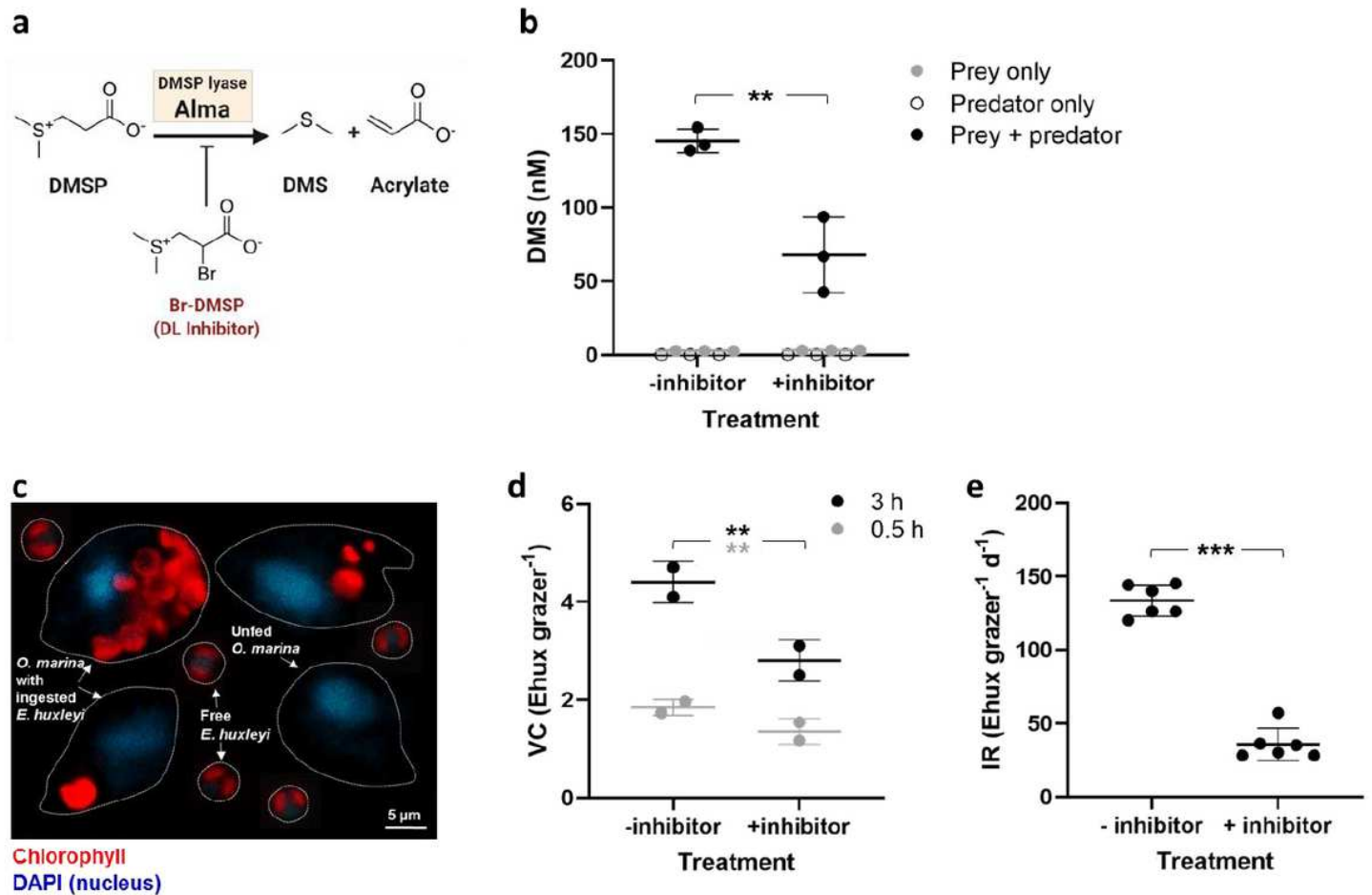


**Figure 1**

Reduced DMSP lyase (DL) activity of *E. huxleyi* impaired grazing by *O. marina*. a, The DMSP lyase Alma cleaves DMSP to DMS and acrylate. The inhibitor Br-DMSP blocks DL activity by forming an enzyme-inhibitor covalent bond at the active site, thus inhibiting the formation of DMS and acrylate. b, The short-term (~1 h) effect of 0.2 μM Br-DMSP on DMS production in-vivo by *E. huxleyi* 373. Horizontal lines represent the mean ± SD; n = 3; P < 0.008 (Student's T-test). c, Fluorescence micrograph collage of *O. marina* with free and ingested *E. huxleyi* cells at t=30 minutes from prey addition. d, The effect of 0.2 μM Br-DMSP on the food vacuole content (VC, *E. huxleyi* 373 cells per grazer) of *O. marina* at t=0.5 and 3 h. A total of 800 *O. marina* cells were examined, 100 cells per biological replicate. Horizontal lines represent the mean ± SD; n = 2; P < 0.003 (generalized linear mixed model). e, The effect of 0.2 μM Br-DMSP on ingestion rate (IR) of *E. huxleyi* 373 cells (Ehux) by *O. marina*, quantified by flow cytometry and based on prey removal from the medium during 50 min. Approximately 2,500 cells were analyzed per sample. Horizontal lines represent the mean ± SD; n = 6; P < 0.0001 (Student's T-test).

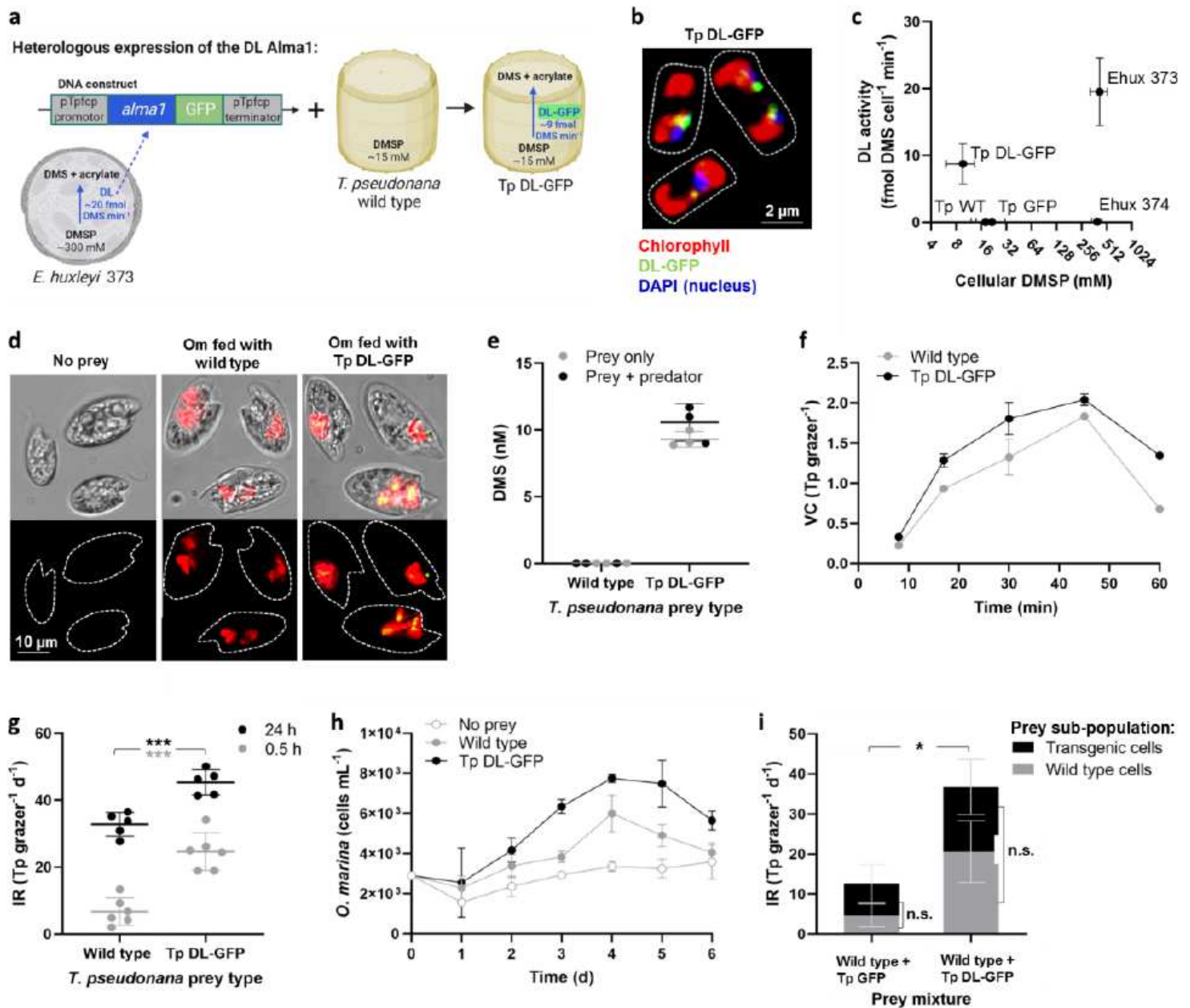


**Figure 2**

Overexpression of DMSP lyase (DL) in algal prey cells enhanced grazing efficiency and growth by *O. marina*. a, Transgenic Tp DL-GFP cells were generated by heterologous expression of the *alma1* gene from *E. huxleyi* 373, fused to GFP, in wild type *T. pseudonana* cells. b, Confocal microscopy of Tp DL-GFP cells. The Alma-GFP protein can be observed as a punctate green signal in close proximity to the chloroplast. c, Intracellular DMSP content and DL activity in *E. huxleyi* (Ehux) strains 373 and 374, as well as in *T. pseudonana* wild type (Tp WT), Tp GFP and Tp DL-GFP. We quantified DL activity in vitro by measuring DMS generation in cell lysates following addition of 10 mM DMSP. Values are mean  $\pm$  SD; n = 3-4. For DMSP, results from two independent measurements were averaged. d, Bright field and fluorescence micrographs of *O. marina* (Om) with ingested *T. pseudonana* cells. e, DMS emission during grazing by *O. marina* on Tp DL-GFP cells. Horizontal lines represent the mean  $\pm$  SD; n = 3. f, Prey uptake curve based on vacuole content (VC) analysis during the first hour of grazing interaction. Values

represent the mean  $\pm$  SD. n = 2-4. A total of 800 grazers were analyzed for t= 8 and 17 min, and 400 grazers for t=30, 45, and 60 min. The mean VC values during 60 min were significantly different between the two prey types,  $P < 0.0001$  (generalized linear mixed model). g, Ingestion rate (IR) analysis based on quantification of *T. pseudonana* (Tp) cell removal from the medium during 0.5 and 24 h of incubation with *O. marina*. Horizontal lines represent the mean  $\pm$  SD; n = 6.  $P < 0.0001$  (Student's T-test). h, Growth dynamics of *O. marina* under starvation conditions or daily feeding with Tp DL-GFP or wild type cells; n = 4. The growth in the Tp DL-GFP treatment was significantly faster than wild type,  $P < 0.0012$  (mixed effects model). i, Double-prey competition trials based on IR analysis of two prey types introduced to *O. marina* in a 1:1 ratio, as measured over 2 h. Values are mean  $\pm$ SD; n = 3-4 in two independent experiments.  $P < 0.001$  when comparing the total IR between the two prey mixtures. When comparing the specific IR on each prey sub-population within a mixture,  $P > 0.32$ , n.s.- not significant (Student's T-test).

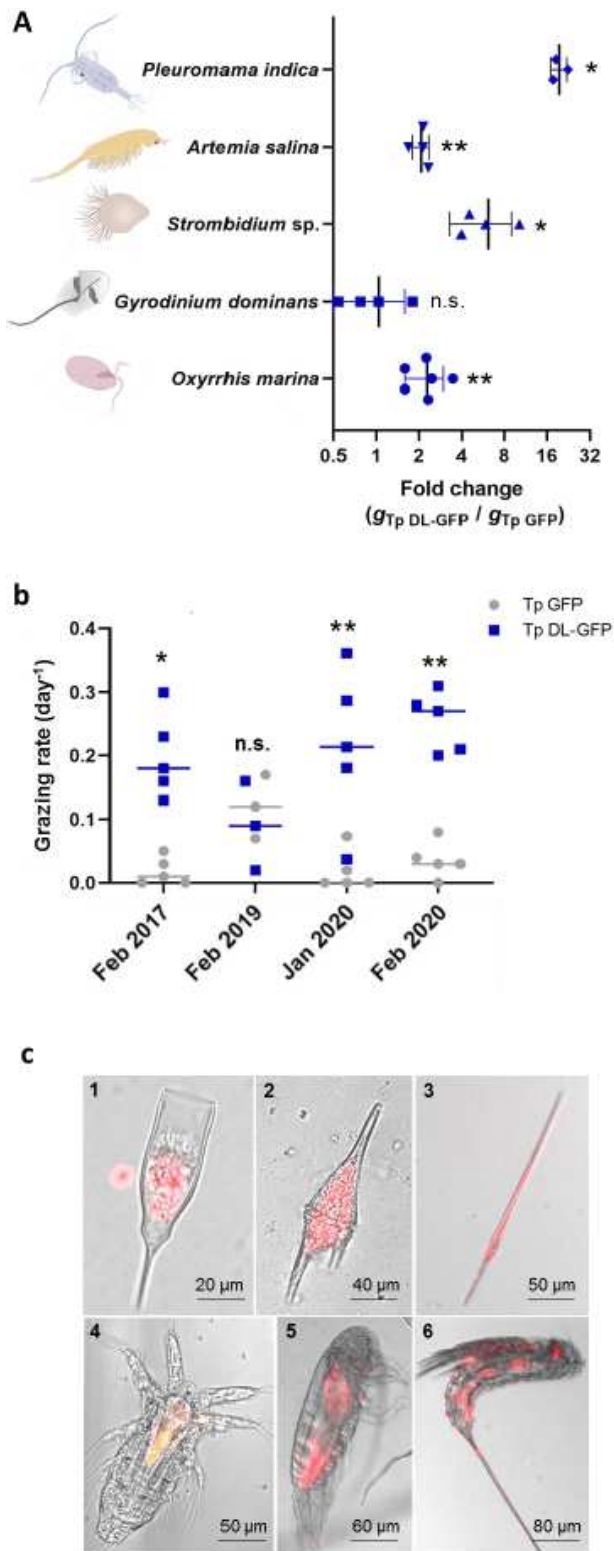


**Figure 3**

Induced DMS production in algal prey enhanced grazing by diverse zooplankton. a, The grazing response of diverse zooplankton fed with Tp DL-GFP cells. Tp GFP cells were used as control prey. The fold change in grazing rate ( $g$ , as assessed by monitoring free prey cells using flow cytometry) on each prey type was calculated, where fold change  $> 1$  indicates faster grazing on Tp DL-GFP cells. Vertical lines represent the mean  $\pm$  SD;  $n = 3$  for *P. indica*; 4 for *A. salina*, *G. dominans* and *Strombidium sp.*; 6 for *O. marina*. n.s.- not

significant,  $P > 0.897$ ;  $*P < 0.011$ ;  $**P < 0.003$  (one-sample T-test). b, Grazing of Tp DL-GFP cells by natural microzooplankton from the Red Sea. Two prey types were offered to the microzooplankton assemblages: Tp GFP or Tp DL-GFP. Horizontal lines represent the mean;  $n=5-6$ .  $*P < 0.017$ ;  $**P < 0.005$  (Student's T-test). c, Variety of wild microzooplankton observed during grazing experiments shown in (b), including tintinnid ciliate (1), mixotrophic Ceratium dinoflagellates (2-3) and diverse copepods (4-6). Red represents the chlorophyll of ingested *T. pseudonana* cells added as prey (mixotrophic dinoflagellates also have endogenous chlorophyll).

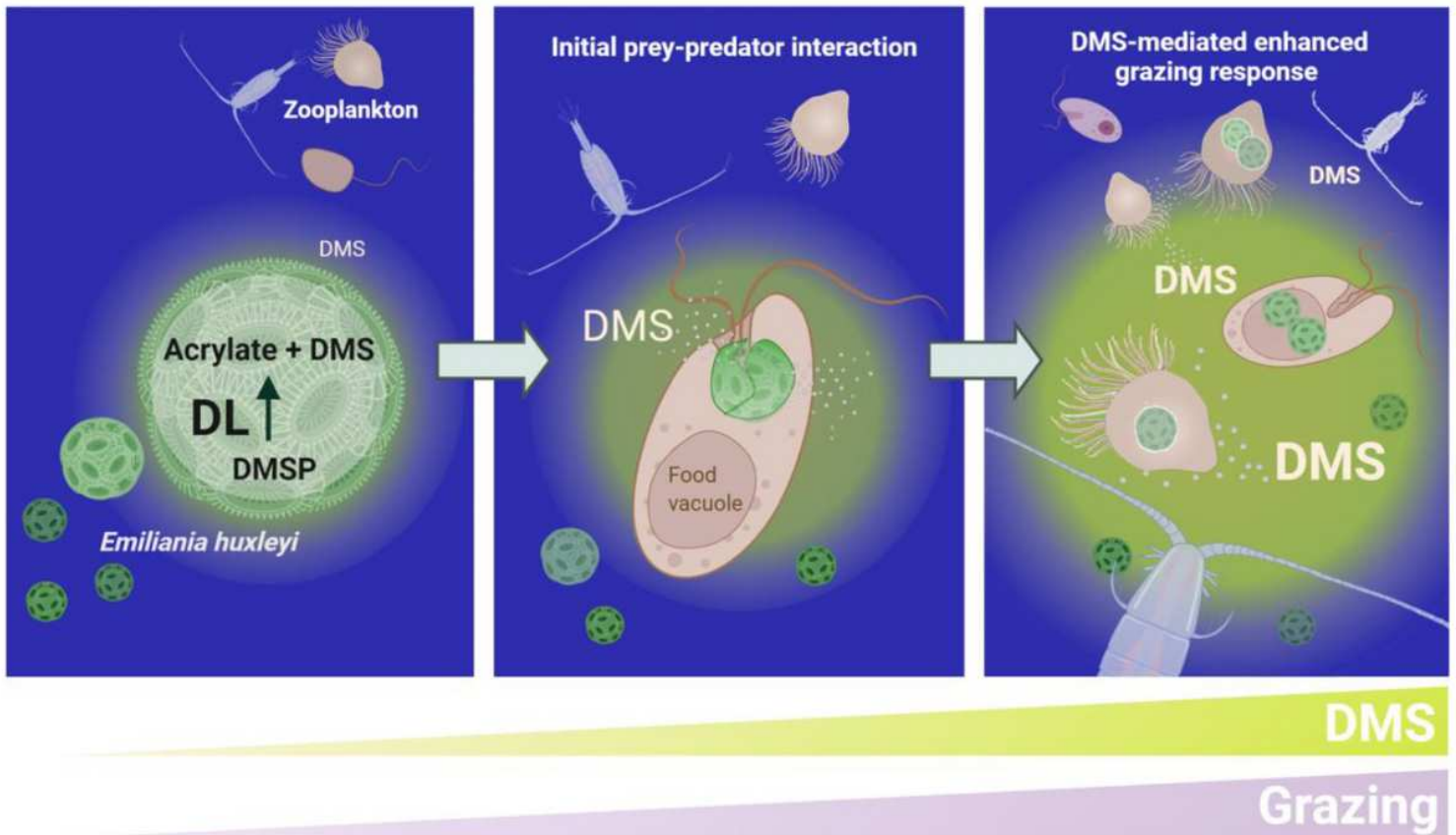


**Figure 4**

The ecological impact of algal DMS on planktonic prey-predator interactions. A conceptual model describing DMS-mediated herbivory. Chemoattraction of zooplankton to leakage of DMS from high DMS producing algae such of *E. huxleyi* cells may facilitate initial grazing interaction (left panel). Upon dissociation of ingested cells during phagocytosis, the DL Alma1 degrades DMSP and releases more DMS into the water (middle panel). This microscale release of DMS may accumulate to high concentration, which induces an increase in the overall grazing pressure by diverse grazers on the entire phytoplankton population (right panel) and thus has wide ecological implication in the marine environment.

## Supplementary Files

This is a list of supplementary files associated with this preprint. Click to download.

- [ShemietalSuppMaterials.pdf](#)